Hybrid Reactive Power Compensator with Adaptation of the Operation of the Control System to the Parameters of the Mains Voltage

Goolak S.[1], Tkachenko V.[1] Kyrychenko M.[2], Kozlov S.[3]
[1]State University of Infrastructure and Technologies
Kyiv, Ukraine
[2]Kyiv National University of Construction and Architecture
Kyiv, Ukraine
[3]National Technical University «Kharkiv Polytechnic Institute»
Kharkiv, Ukraine

Abstract. The aim of the work is to develop a model of a hybrid reactive power compensator with adaptation of the control system to the parameters of the voltage supply. The task was achieved by applying the control algorithm for the operation of the control system of the active part of the reactive power compensator, which is based on the regression analysis method. The traction drive of the AC electric locomotive VL-80K, which is operated on the railways of the Ukraine, was chosen as the object of study. The simulation of the traction drive operation was carried out for a traction drive with and without a reactive power compensator, for cases where the process of changing the voltage in the catenary was a stationary deterministic process and for the case when this process was a non-stationary non-deterministic process. The most important result is the development of a block diagram of the control system for the active part of the reactive power compensator based on the implementation of the Levinson-Durbin linear prediction algorithm. The significance of the results obtained lies in the possibility of the proposed control scheme for the active part of the compensator to adapt the operation of the compensator to the voltage parameters of the catenary, that is, to the actual operating conditions of the electric locomotive.
***Keywords*:** active power, reactive power, apparent power, reactive power compensation, traction drive, electric locomotive, control system.
DOI: https://doi.org/10.52254/1857-0070.2023.1-57.01
UDC: УДК 621.316.722.076.12

Compensator hibrid de putere reactivă cu adaptare a funcționării sistemului de control la parametrii tensiunii de rețea

Gulac S.A.[1], Tkacenko V.P[1], Kiricenko M.A.[2], Kozlov S.S.[3]
[1]Universitatea de Stat de Infrastructură și Tehnologie, Kiev, Ucraina
[2]Universitatea Națională de Construcții și Arhitectură din Kiev, Kiev, Ucraina
[3]Universitatea Națională Tehnică «Institutul Politehnic din Kharkiv», Harkov, Ucraina
Rezumat. Scopul lucrării este elaborarea unui model al compensatorului hibrid de putere reactivă cu adaptarea sistemului de control la parametrii tensiunii de alimentare. Sarcina a fost realizată prin aplicarea algoritmului de control pentru funcționarea sistemului de dirijare al părții active a compensatorului de putere reactivă, care se bazează pe metoda analizei regresiei. Ca obiect de studiu a fost ales sistemul de tracțiune al locomotivei electrice AC VL-80k, care este operată pe căile ferate din Ucraina. Simularea funcționării tracțiunii a fost efectuată pentru o unitate de tracțiune cu și fără un compensator de putere reactivă, pentru cazurile în care procesul de modificare a tensiunii în rețeaua de contact a fost un proces staționar determinat și în cazul unui proces nestaționar nedeterminat. Cel mai important rezultat este elaborarea diagramei bloc a sistemului de control pentru partea activă a compensatorului de putere reactivă bazată pe implementarea algoritmului de predicție liniară Levinson-Darbin. Semnificația rezultatelor obținute constă în posibilitatea schemei de control propuse pentru partea activă a compensatorului de a adapta funcționarea compensatorului la parametrii de tensiune ai rețelei de contact, adică la condițiile reale de funcționare a locomotivei electrice. Utilizarea unui compensator hibrid de putere reactivă cu adaptarea sistemului de control al părții active la parametrii de tensiune ai rețelei de contact a făcut posibilă creșterea factorului de putere al locomotivei electrice și, ca urmare, reducerea puterii totale consumate de către locomotiva electrica din reteaua de contact.
***Cuvinte-cheie*:** putere activă, putere reactivă, putere aparentă, compensare putere reactivă, tracțiune, locomotivă electrică, sistem de control.

Гибридный компенсатор реактивной мощности с адаптацией работы системы управления к параметрам напряжения питающей сети

Гулак С.А.[1], Ткаченко В.П.[1], Кириченко М.А.[2], Козлов С.С.[3]
[1]Государственный университет инфраструктуры и технологий, Киев, Украина
[2]Киевский национальный университет строительства и архитектуры, Киев, Украина
[3]Национальный технический университет «Харьковский политехнический институт», Харьков, Украина

Аннотация. Целью работы является разработка модели гибридного компенсатора реактивной мощности с адаптацией работы системы управления к параметрам напряжения питающей сети. Поставленная задача была достигнута путем применения алгоритма управления работой системы управления активной частью компенсатора реактивной мощности, в основе которого лежит метод регрессионного анализа. В качестве объекта исследования был выбран тяговый привод электровоза переменного тока ВЛ-80к, который эксплуатируется на железных дорогах Украины. Моделирование работы тягового привода проводилось для тягового привода с компенсатором и без компенсатора реактивной мощности, для случаев, когда процесс изменения напряжения в контактной сети являлся стационарным детерминированным процессом и для случая, когда этот процесс являлся нестационарным недетерминированным процессом. Наиболее важным результатом является разработка структурной схемы системы управления активной частью компенсатора реактивной мощности на основе реализации алгоритма линейного прогнозирования Левинсона-Дарбина. Значимость полученных результатов состоит в возможности предложенной схемы управления активной частью компенсатора адаптировать работу компенсатора к параметрам напряжения контактной сети, то есть к реальным условиям работы электровоза. Применение гибридного компенсатора реактивной мощности с адаптацией системы управления активной частью к параметрам напряжения контактной сети позволило повысить коэффициент мощности электровоза и, как следствие, уменьшить полную мощность, которая потребляется электровозом с контактной сети. Результаты моделирования показали, что наибольший эффект о применения гибридного компенсатора реактивной мощности имеет место в условиях нестационарного недетерминированного процесса изменения напряжения контактной сети.

Ключевые слова: активная мощность, реактивная мощность, полная мощность, компенсация реактивной мощности, тяговый привод, электровоз, система управления.

INTRODUCTION

The system of the traction electric supply is one most powerful load of the public network. They have serious problems with the electric energy quality. Various topologies of the supply for these systems resulted in substantial quantity of the types of distortions in the network voltage and current in the system of the traction electric supply, united energy system and neighboring consumers [1]. The operational process of the electric rolling stock leads to occurrence of nonsymmetric currents, voltage falls in the catenary, overvoltage, high-order harmonics of voltage components in the catenary [2]. Increase in these factors' impact on the form of voltage in the catenary enlarges the losses and decreases the power coefficient, i.e., reduces the quality indices of the electric energy system of the traction electric supply. This fact increases the cash accounts, which the infrastructure managers must pay to the operator, who supplies the electric energy to the railway system [3].

The most powerful electric energy consumer in their traction electric supply system is the electric rolling stock. It is this transportation mode that introduces the highest distortions into the system of the traction electric supply, which decrease the indices of quality of the traction electro-supply system. These distortions are caused by the:

- phase shift between the voltage of the catenary and the traction current;
- generation the voltage super harmonic components into the catenary by the electric rolling stock;
- condition of passing the feeder zone by the electric rolling stock;
- the presence of several units of the electric rolling stock at a single feeder zone;
- quality of current collection;
- change in the modes of work of the electric rolling stock [4-6].

To remove the negative factors that influence on the distortions of the quality indices of the traction electric supply system, the electric locomotive is equipped with the reactive power compensators [7, 8]. The reactive power compensators can be realized as:

- passive filters [9, 10];
- active filters [11, 12];
- hybrid filters (combination of passive and active filter) [13, 14].

To remove the phase shift between the voltage of the catenary and the traction current, the passive filters are the most efficient [9, 10]. However, for the inhibition of the super harmonic components of the traction current, these filters are inefficient, since they are adapted just for a definite frequency [13, 14]. The active filters are efficient for the inhibition of the super harmonic components of the traction current [11, 12], however, they are inefficient in removing the phase shift between the catenary voltage and traction current [13, 14]. The efficient for the reactive power compensation on the electric locomotive are the hybrid compensators [7, 8]. The passive compensator part, which is the LC-filter, that removes the phase shift between the catenary voltage and traction current, and the active part of the compensator, which is an independent inverter of voltage, generates into the circuit of the secondary winding of the traction transformer the super harmonic components of the traction current in a counter phase to those existing [7, 8]. In this context, the algorithm of the work of the control system of the independent voltage invertor is constructed based on the analysis of the super harmonic components of the traction current. The analysis of the super harmonic components of the traction current is performed based on the algorithm of the Fourier fast transformation [15].

The process of the voltage change in the catenary is nonstationary, nondeterministic, non-gaussian process [16, 17]. This fact is resulted from the operation modes of the electric rolling stock[18]. In conditions when the process of changing the controlled parameter is nonstationary, nondeterministic, non-gaussian, the Fourier transformation algorithms application to it is incorrect [19, 20].

For the spectral analysis under conditions, when the process of changing the controlled parameter is nonstationary, nondeterministic, non- gaussian, there is a good reason to use the algorithms of a correlation analysis [21, 22].

Since the voltage change in the catenary is a non-gaussian process, it is reasonable to use the methods of nonlinear prediction when carrying out the correlation analysis [23]. In [23], the system of monitoring by the active part of the reactive power compensator was offered based on the modified autoregressive method. Regardless of high speed of the compensator operation and high level of inhibition of the high-order harmonics components of the traction current, the introduction of additional double integration into the system decreases the system tolerance.

In [18], the Levinson-Durbin algorithm is proposed for the realization of the compensator monitoring system of the reactive power. Low speed of operation is the disadvantage of this method. However, in the track electric-supply systems the process of changing voltage in the catenary is not a speedy process from the viewpoint of signals' digital processing methods.

The advantages of the method are high stability and the possibility to process large bulk of data [18]. However, in [18], this method was realized conceptually.

In this work, the system of monitoring by the active part of the hybrid compensator of the reactive power that allows the reactive power to be compensated in conditions of nonstationary, nondeterministic, non-gaussian process of voltage change in the network.

The realization of the monitoring system is performed based on the algorithm of the Levinson-Durbin linear prediction, which made it possible to carry out the monitoring by the compensator power part with a high stability and operate using a large data bulk.

The results of this work can be used when designing the reactive power compensators, which are introduced into the traction driver of the AC electric locomotive.

The aim of this research is to create a model of a reactive power hybrid compensator for the traction drive of the AC electric locomotive with taking into account the real conditions of the electric locomotive operation.

This work is distinguished by the fact that during the development of the model of the system for the monitoring by the active part of the hybrid power compensator, the Levinson-Durbin linear prediction algorithm was proposed to determine the high-order harmonic components of the traction current.

This allowed the possibility of the high-order harmonic traction current components to be to compensated in conditions of the nonstationary, nondeterministic, non-gaussian process of changing voltage in the catenary.

In addition, the use of the of the proposed model of the system for the monitoring by reactive power compensator active part, allowed considering the real conditions of the electric locomotive exploitation during the compensator operation.

DEVELOPMENT OF STRUCTURAL ARRANGEMENT OF MONITORING

SYSTEM USING REACTIVE POWER COMPENSATOR

The traction drive of the VL-80K AC locomotive that is used for the Ukrainian railway lines was accepted as the object for the research. The technical characteristics of the track drive of the VL-80k AC locomotive are shown in Table 1.

Table 1

VL-80K AC locomotive traction drive technical characteristics

Parameter	Designation	Unit of measurement	Value
Total power of initial (of network) traction winding of transformer	S_1	kVA	4485
Nominal voltage of traction transformer primary winding	U_1	V	25000
Nominal current of primary traction winding	I_1	A	245
Frequency of supply voltage	f	Hz	50
Nominal voltage of secondary traction winding of transformer	U_2	V	1218
Nominal current of secondary winding of traction transformer (1 section) in continuous service	I_2	A	1750
Number of traction locomotives in one section	k		4
Nominal rotation frequency of motor shaft	n	rpm	915
Nominal power coefficient of locomotive including drive of supporting machines	k_p	Ohm	0,866
Nominal coefficient of efficiency considering supporting machines drive	η	%	84

All the rest studies will be performed under condition that the drive of the supporting machines of the locomotive will be disconnected.

The mathematical model of the active part of the hybrid filter was based on its calculation scheme (Fig. 1) [24]. Transistors VT1-VT4 and diodes VD1-VD4 form the scheme of the four-quadrant converter connected to the source of the alternative voltage u_2 (the transformer secondary winding) via the smoothing choke L_a. The DC circuit of the active filter is modeled by the voltage source, whose internal voltage is r_a.

As to its circuit simulation, the converter is an autonomous inverter of voltage (AIV) with a voltage pulse-width modulation (PWM). The scheme of a four-quadrant converter are two back-to-back bridge rectifiers: monitored VT1-VT4 and uncontrolled VD1-VD4, connected on the side of the clamp-locks of the alternative voltage.

These points are connected with an output source of the alternative voltage u_2.

The input voltage in the form of the EMF Ed is switched on between the anodic and cathode groups of the uncontrolled VD1-VD4 rectifier. The principle of the converter operation suggests including inductance L_a into the source circuit u_2.

Switching on and off of the VT1 and VTI4 transistors of the converter is performed according to the law that ensures the pulse-width modulation of voltage according to the form of modulating voltage.

Monitoring voltage for VT1-VT4 is formed using the controlling system by comparison of two signals: modulation voltage u_M and generator voltage of sawtooth voltage u_{GSTV} (Fig. 2).

Generator frequency $f_{GSTV} = k \cdot f_m$ must be odd-multiple to the frequency of source u_2. Figure 2 shows the diagram voltages and currents relative to work $4qS$ - of converter with $k = 9$.

Pulses monitoring transistors VT1-VT4 are formed now of equality of voltages u_M and u_{GSTV} and correspond to the following logical functions (1):

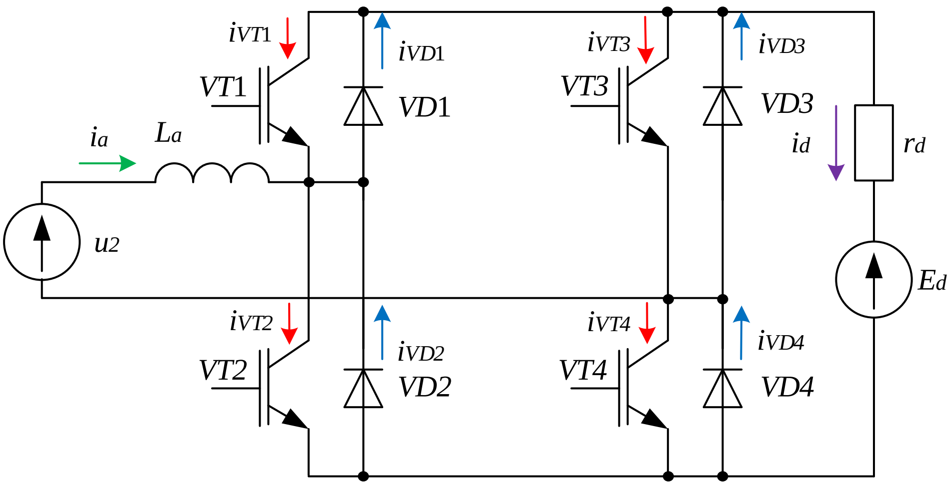

Fig. 1. Calculation scheme for the active filter.

$$VT1 = \begin{cases} 1 & if \quad u_M - u_{GSTV} \geq 0, \\ 0 & if \quad u_M - u_{GSTV} < 0, \end{cases},$$
$$VT2 = \begin{cases} 1 & if \quad -u_M - u_{GSTV} \geq 0, \\ 0 & if \quad u_M - u_{GSTV} < 0, \end{cases}, \qquad (1)$$
$$VT3 = \overline{VT1}, \quad VT4 = \overline{VT2}.$$

According to Fig. 2, upon switching on diagonal transistors VT1 and VT4 (VT2, VT3), voltage u_{11} is formed on the clamps of the alternative current converter with amplitude ±Ed and which is regulated using the law of modulating voltage u_m. Voltage phase u_{11} depends on the phase u_m u_m relatively source voltage u_2 and E_d the current in circuit i_a can be determined using the following formula:

$$L_a \cdot \frac{di_a}{dt} = u_2 - u_{11}. \qquad (2)$$

At connecting the adjacent elements (e.g, VT3 and VD1), the current contour is formed, which is closing via the back valve VD1 and transistor VT3. Upon that, source E_d is disconnected from the converter by the closed transistors VT2, VT4, therefore the voltage at the clamps of the alternative current u_{11}, as well as the current, equal to zero. The converter output current i_a is restricted by the inductance L_a, at $u_{11} = 0$ is expressed using the following expression:

$$L_a \cdot \frac{di_a}{dt} = u_2. \qquad (3)$$

At $di_a / dt > 0$, increase in the current i_a and energy accumulation in inductance L_a occur.

Figure 2 shows that the output current i_a looks like as a zigzag line consisting of growing and decreasing sections.

The degree of the smoothing current is defined by inductance L_a of the input source, as well as the frequency of the saw tooth voltage u_{GSTV}. The increase in these values makes i_a form to be smoother. The system of equations composed in accordance to the first and second Kirchhoff laws for the system presented in Fig. 1 looks like as follows:

$$\begin{aligned}
& i_{VD1} + i_{VD3} - i_{VT1} - i_{VT3} - i_d = 0, \\
& i_{VT1} + i_{VD2} - i_{VT2} - i_{VD1} + i_d = 0, \\
& i_{VT2} + i_{VT4} - i_{VD2} - i_{VD1} + i_d = 0, \\
& i_{VT1} \cdot r_{VT1} + i_{VD1} \cdot r_{VD1} = 0, \\
& i_{VT2} \cdot r_{VT2} + i_{VD2} \cdot r_{VD2} = 0, \\
& i_{VT3} \cdot r_{VT3} + i_{VD1} \cdot r_{VD1} + L_a \cdot \frac{di_a}{dt} = u_2, \\
& i_{VT4} \cdot r_{VT4} + i_{VD2} \cdot r_{VD2} + L_a \cdot \frac{di_a}{dt} = u_2, \\
& i_{VT3} \cdot r_{VT3} + i_{VD3} \cdot r_{VD3} = 0, \\
& i_{VT4} \cdot r_{VT4} + i_{VD4} \cdot r_{VD4} = 0, \\
& i_{VT3} \cdot r_{VT3} + i_{VD4} \cdot r_{VD4} + i_d \cdot r_d = -E_d.
\end{aligned} \qquad (4)$$

In equations 4 there are: $r_{VT1} - r_{VT4}$, $r_{VD1} - r_{VD4}$ – relevant to resistances of transistors VT1-VT4 and diodes VD1-VD4, u_2 is the voltage of the transformer secondary winding, E_d is the voltage in the circuit of the rectified current, $i_{VT1} - i_{VT4}$, , $i_{VD1} - i_{VD4}$, i_a and i_d are the branch currents.

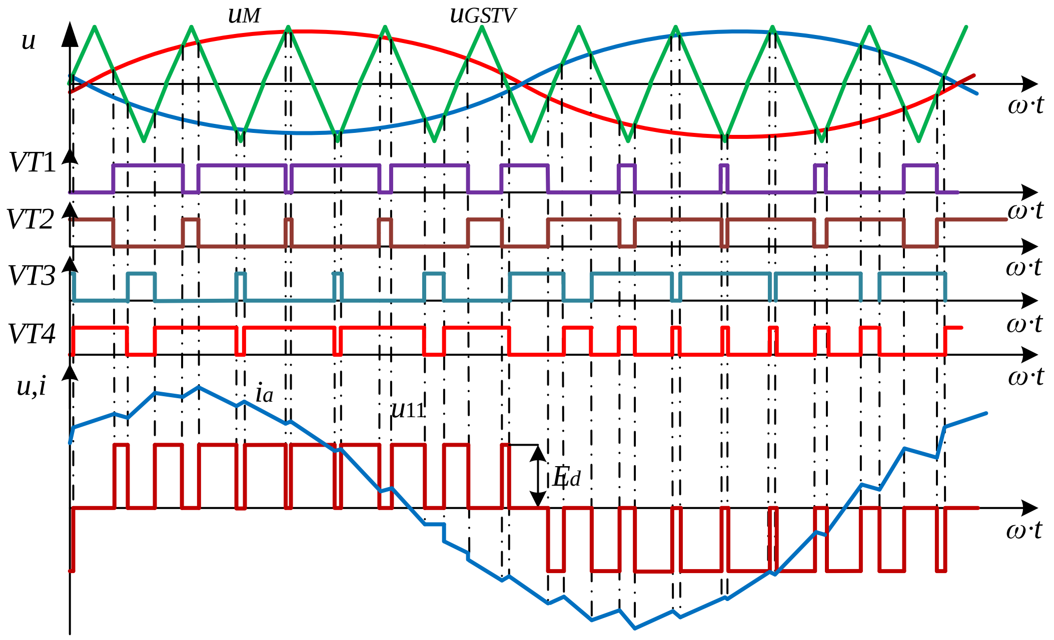

Fig. 2. Diagrams of currents and voltages that explain the voltage autonomous inverter operation.

In [18] it was noted that one method for the construction of the system for monitoring by the active part of the reactive power compensator can be the system, whose operation is adapted to the form of the current, which is passing in the secondary winding of the traction transformer (for instance, the monitoring scheme exhibited in Fig. 3).

The operation principle of this scheme is as follows. Using a current sensor, the value of the passing current is measured in the circuits of the secondary winding of the traction transformer. The measurements are performed discretely. The discrete values, using the analogue-digital convertor (ADC), turn into the binary code and are supplied to the harmonic components evaluator, where the spectral components of the amplitude-frequency $A_{I2}(\omega)$ and phase-frequency $\varphi_{I2}(\omega)$ are calculated. In the block of selection of high spectral components, all of the spectral components like the amplitude-frequency and phase-frequency spectrum, except for the first harmonics, are multiplied by unity. The spectral components of the first harmonics are multiplied by zero.

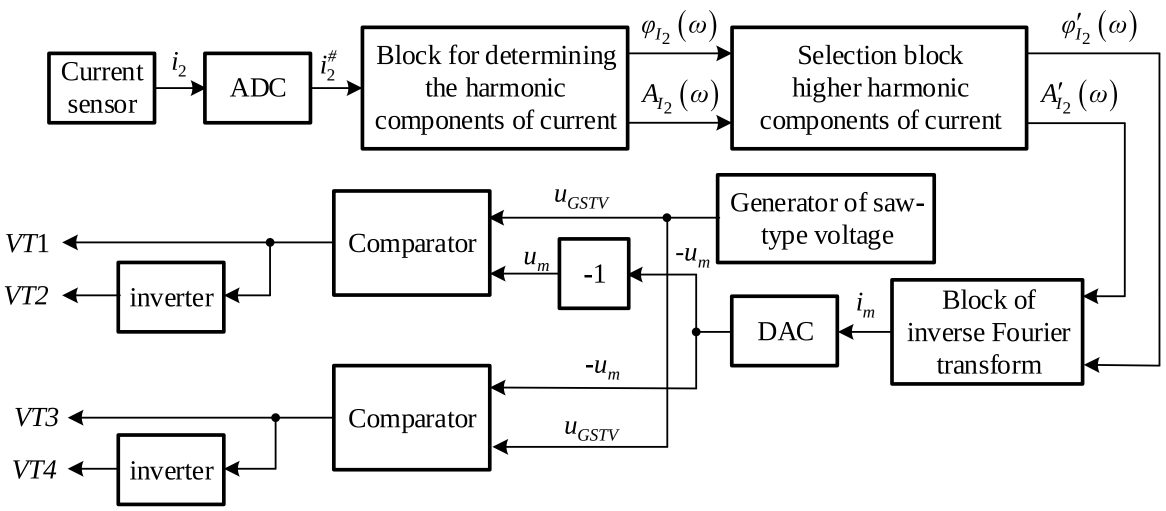

Fig. 3. Monitoring scheme of the active part of reactive power compensator.

After this the inverse Fourier transformation is fulfilled for the purpose of obtaining the current modulation curve i_m. The current of modulation is supplied to the digital-analogous converter (ADC), which transforms the current from the digital into analogous form. Since to obtain the modulation current curve from the power circuit current, it is necessary to subtract the obtained current value (the scheme designates it as u_m). To realize the pulse-duration modulation (PDM) according to Fig. 2, it is necessary to have two channels. One channel that works with a direct form of modulation signal, realizes the laws of monitoring for transistors VT1 and VT2. The second channel that works with a modulation signal form, whose phase differs by π radian from the direct form of modulation signal, realizes the laws of monitoring for transistors VT3 and VT4. For this purpose, the direct modulation signal - u_m, which realizes the monitoring law for transistors VT1 and VT2 at the output of the ADC, is multiplied by -1 and is supplied into the comparator where it is compared with the voltage of the saw-type generator u_{GSTV}. For transistors VT3 and VT4, the modulation signal is fed to the other comparator, where it is compared to the generator voltage of the saw-type voltage u_{GSTV}. At the outputs of the comparators, the monitoring pulses are formed by transistors VT1 and VT3.

According to equations (1), the monitoring signals for transistors VT2 and VT4 are inversions of the monitoring signals for transistors VT1 and VT3. On the scheme, this operation is fulfilled by the invertor, which inverts the monitoring signals' values for transistors VT1 and VT3, correspondingly.

- using the linear prediction filter the output value, which in this case is the power circuit current of the traction drive, turns from the random nonergodic value into the ergodic value, which can be applicable to the discrete Fourier transformation;
- the discrete Fourier transformation allows determining the components of the amplitude-frequency and phase-frequency spectrum.

Исходя из вышеизложенного, структурная Based on the aforementioned, the structural scheme of the block of determination the harmonic components looks like as shown in Fig. 4.

Since the input current at the output of the analogue-digital converter is a discrete value in time, we can introduce the following designation:

$$i_2^{\#}(t) = i_2^{\#}(nT) = i_2^{\#}(n) = x(n). \qquad (5)$$

where T is the discretization period; n is the account number.

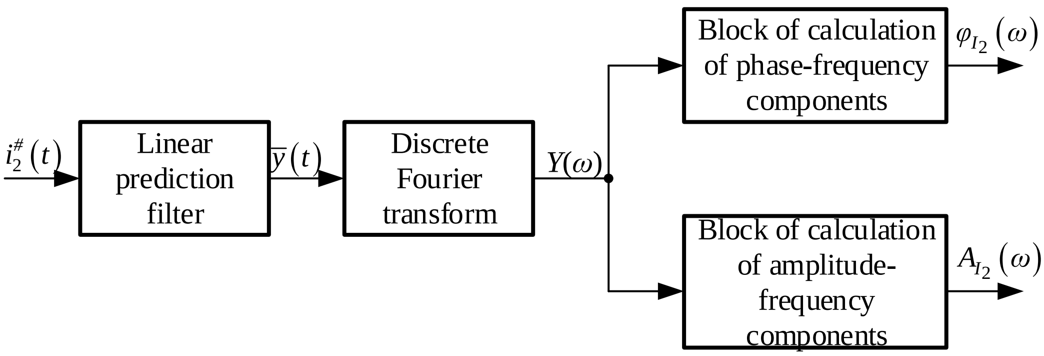

Fig, 4. Structural scheme of the block for harmonic components' definition.

The essence of the method for definition of the spectral components of current and voltages in the traction drive circuits of the AC locomotives for the scheme offered (Fig. 4) consists in the following [18]:

-the statistical series of the input data x(n) is applicated with the L length Hamming window;

-the equation system is arranged for the input data of x(n), whose matrix form of the record is:

$$\mathbf{R} \cdot \mathbf{a} = \mathbf{r}, \qquad (6)$$

where **R** is the symmetrical matrix of coefficients;

a is the vector of parameters of linear prediction; **r** is the vector of free terms.

The elements of symmetric matrix of the coefficients are calculated using formula (7):

$$\sum_{l=1}^{L} x(l-k) \cdot x(l-i) = R_{ik}, \qquad (7)$$

where k is the column number;

1 is the line number.

The elements of the vector free terms are calculated using formula (8):

$$\sum_{l=1}^{L} x(l)\cdot x(l-i)=R_i. \quad (8)$$

- the order of prediction K is selected, and the obtained equation system is used to separate the first block with a size of $K-1$;

– for each equation of the first block of data, the coefficients of the prediction filter $a_k^{(i)}$ are calculated using the Levinson-Durbin method.

The initial conditions are preset

$$E_0=R_0, \quad (9)$$

where E_0 is the initial mean quadratic error of the linear prediction.

Gradually, at a step of iteration $i\ (i=1,2,\ldots,K)$ the calculations are performed using the recurrent formulas (10-13):

$$r_i=\frac{\sum_{k}^{i-1} a_k^{(i-1)}\cdot R_{i-k}}{E_{i-1}}; \quad (10)$$

$$a_k^{(i)}=r_i; \quad (11)$$

$$a_k^{(i)}=a_k^{(i-1)}-r_i\cdot a_{i-k}^{(i-1)},\quad 1\le k\le i-1; \quad (12)$$

$$E_i=\left(1-r_i^2\right)\cdot E_{i-1}. \quad (13)$$

-prediction is increased by 1 with each step, as long as it achieves the value of K;

-the output signal value is calculated using formula

$$\bar{y}(n)=\sum_{k=1}^{K} a_k^{(i)}\cdot x(n-k). \quad (14)$$

-the transition to the next block of data by increasing the line index by 1 of each equation;

-for each equation of the data block the prediction filter coefficients $a_k^{(i)}$ are calculated by the Levinson-Durby method. The value of the output signal is calculated by (14) only for the last equation of the block;

-the quantity of the blocks processed will be L-K-1;

-the spectral components are defined for the obtained series of stationary determinate output signals using the discrete Fourier transformation

$$\bar{Y}(k)=\sum_{n=0}^{L-1}\bar{y}(n)\cdot e^{-j\cdot n\cdot k\cdot\frac{2\cdot\pi}{L}}, \quad (15)$$

where k is the harmonic component number; $\bar{Y}(k)$ is the value of harmonic component in a complex form.

-the components of the amplitude-frequency (16) and phase-frequency (17) spectrum are calculated:

$$A_{I_2}(k)=mod\left(\bar{Y}(k)\right), \quad (16)$$

$$\varphi_{I_2}(k)=arg\left(\bar{Y}(k)\right). \quad (17)$$

-to obtain the monitoring signal the inverse Fourier transformation is necessary to perform

$$i_m(n)=\frac{1}{K}\cdot\sum_{n=0}^{L-1} A_{I_2}(k)\cdot e^{j\varphi_{I_2}(k)}\cdot e^{jn\cdot k\cdot\frac{2\cdot\pi}{L}}. \quad (18)$$

Since to realize the algorithm of operation of the reactive power compensator monitoring system, the recurrent formulas are used, during the development of the imitation model the monitoring system is simpler to realize as the program block.

DEVELOPMENT OF MODEL OF VP-80K LOCOMOTIVE TRACTION DRIVE WITH REACTIVE POWER COMPENSATOR

The scheme of connection the hybrid compensator with AC locomotive power network is shown in Fig. 5 [24].

The simulation model of the reactive power hybrid compensator is carried out in the MATLab program medium. The power part, which realizes scheme of (Fig. 5), is performed using the elements of the library Simscape/Electrical/Specialized Power Systems. The monitoring system is realized using the program from which the monitoring signals are supplied into the power part by transistors VT1-VT4. The simulation model reactive power compensator is combined into block “Reactive power compensator” (Fig. 6).

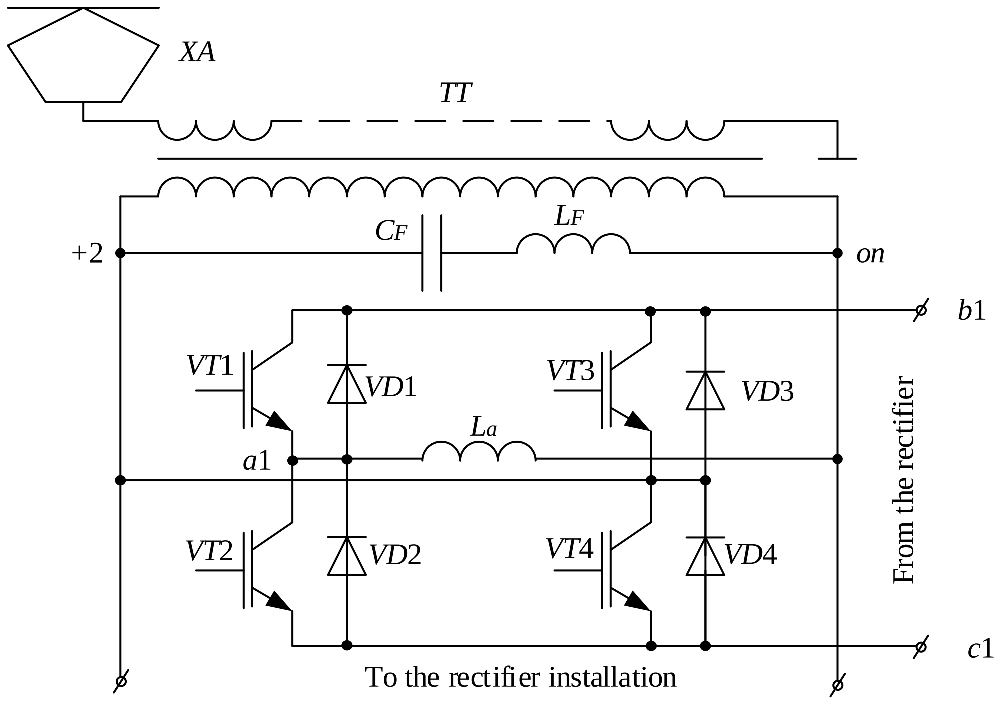

Fig. 5. Scheme of connection the hybrid filter to VL-80K locomotive.

In the work (Goolak et al. System Model Traction substation-contact network-traction drive of the VL-80K series electric locomotive. *Collection of scientific papers of the State Economic and Technological University of Transport. Series: Transport systems and technologies*, 2016, vol. 28, pp. 99-109. irbis-nbuv.gov.ua), the simulation model of the traction drive of VL80K electric locomotive is described. In this work, one section of the electric locomotive has two sections of the secondary winding of the traction transformer x1-o1 and x2-o2. Therefore, the simulation model has two compensators of the reactive power “Reactive power compensator 1” and “Reactive power compensator 2”. The simulation model of the traction drive of one section of the electric locomotive with the reactive power compensators is shown in Fig. 6. All studies were carried out for the nominal mode of operation of the traction electric drive, which corresponds the 28th position of the machinist controller.

The elements of the passive part of the hybrid reactive power compensator are calculated based on the following reasons.

The filter condenser capacity is defined by the reactive power, consumed by the load and calculated using the following ratio [25]:

$$C_f = \frac{Q_{nom}}{2\cdot\pi\cdot f_1\cdot U_C^2} = \frac{1066\cdot 10^3}{2\cdot\pi\cdot 50\cdot 620^2} = 8827, \mu F, \quad (19)$$

where f_1=50 Hz is the frequency of the main voltage harmonics on the secondary winding of the traction transformer;

U_C=U_2=1218 V is the voltage across the condenser (Table.1);

Q_{nom} is the nominal value of the reactive power

$$Q_{nom} = I_2\cdot U_2\cdot\sqrt{1-k_p^2} = \\ = 1750\cdot 1218\cdot\sqrt{1-0,866^2} = 1066, kVAr, \quad (20)$$

where I_2=1750 A is the current of the first harmonics of the second winding of the traction transformer (Table 1);

k_p=0,866 is the power coefficient of the secondary winding of the traction transformer (Table 1).

According to the obtained value of the condenser capacity, the necessary value of the choke inductance was established, satisfying the condition of voltage resonance at a frequency of the first voltage harmonics on the secondary winding of the traction transformer.

Power Systems and entered the blocks of “Reactive power compensator1” and “Reactive power compensator2”.

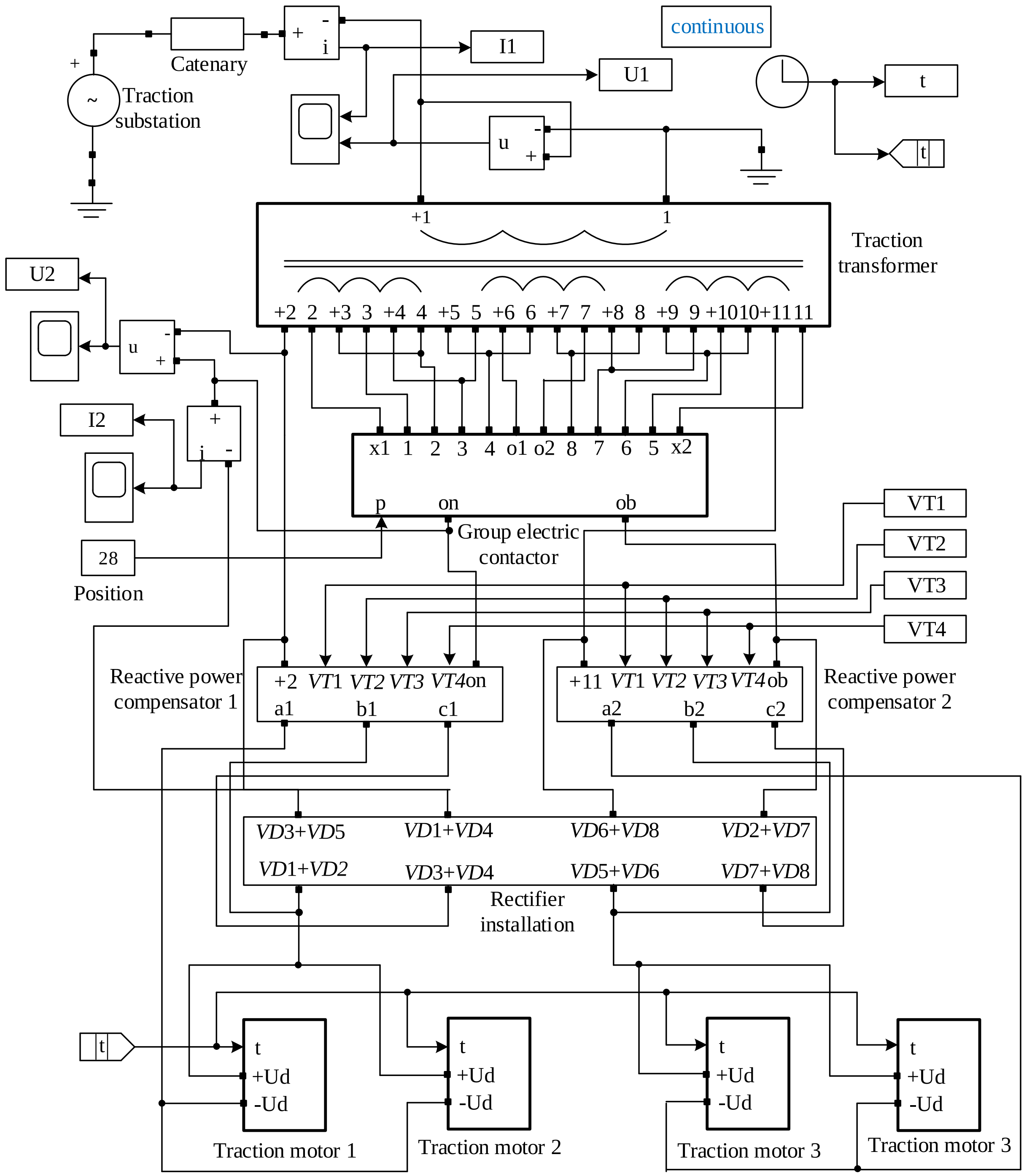

Fig. 6. Single-section traction drive model for VL-80K locomotive with reactive power compensator

$$L_f = \frac{1}{(2\cdot\pi\cdot f_1)^2\cdot C_f} = \qquad (21)$$

$$= \frac{1}{(2\cdot\pi\cdot 50)^2\cdot 2287\cdot 10^{-6}} = 4,44, mH.$$

The elements of the passive filter at the simulation model are realized on the elements of the library Simscape/Electrical/Specialized

RESULTS OF MODELING

At the simulation model (Fig.6) four experiments were carried out. The first experiment consisted of reading the time diagrams of voltage and current on the primary winding of the traction transformer (Fig. 7) in the absence of the reactive power compensator and under condition that the process of changing is of a stationary deterministic character.

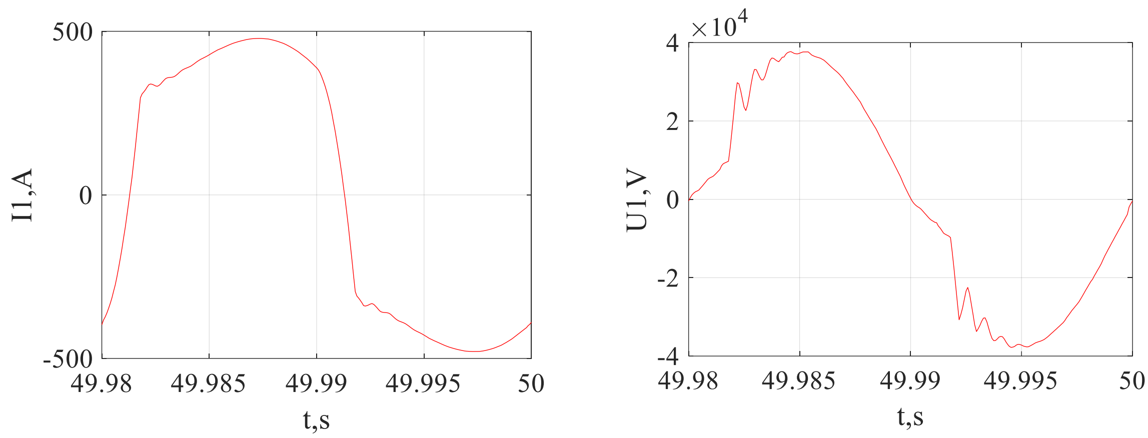

a) b)

Fig. 7. Time diagrams of current (a) and voltage (b) on the primary winding of the traction transformer obtained during the first experiment.

The second experiment consisted in taking the time diagrams of voltage and current on the primary winding of the traction transformer (Fig. 8) with the reactive power compensator and under condition that the process of changing is of a stationary deterministic character.

The third experiment consisted in taking the time diagrams of voltage and current on the primary winding of the traction transformer (Fig. 9) without the reactive power compensator and under condition that the process of changing is of a nonstationary nondeterministic character. For the task of the nonstationary nondeterministic process on the primary winding of the traction transformer in addition to the voltage of the catenary the interferences of the type of a “white noise” were supplied with a dispersion of 5000 V. For the conditions analogous to the third experiment there was a forth experiment. Unlike the third experiment, into the composition of the track drive, the reactive power compensator was introduced. The diagrams of the current and voltage at the primary winding of the track transformer are shown in Fig. 10.

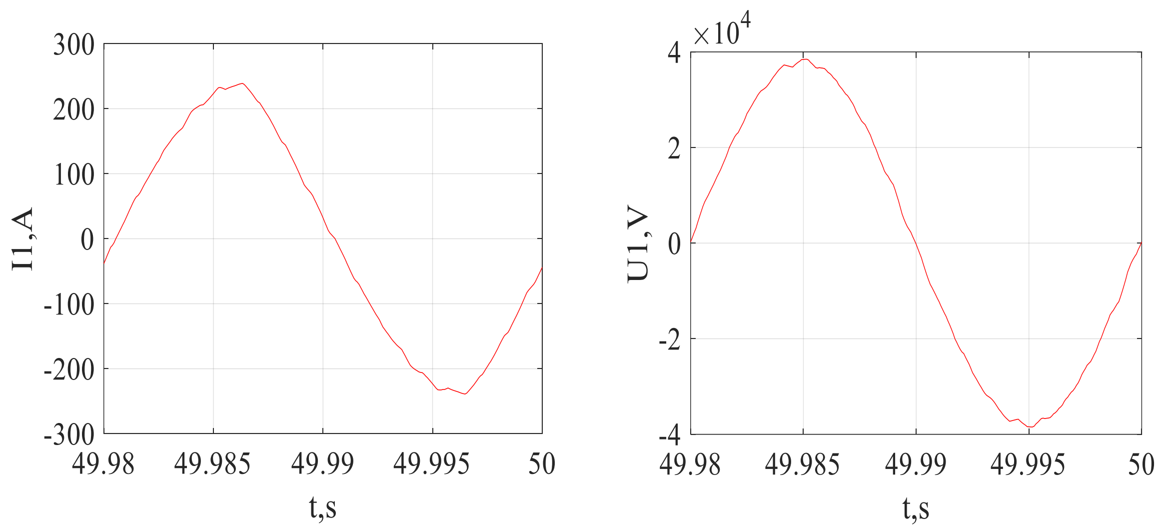

a) b)

Fig. 8. Time diagrams of current (a) and voltage (b) on the primary winding of the traction transformer obtained during the second experiment.

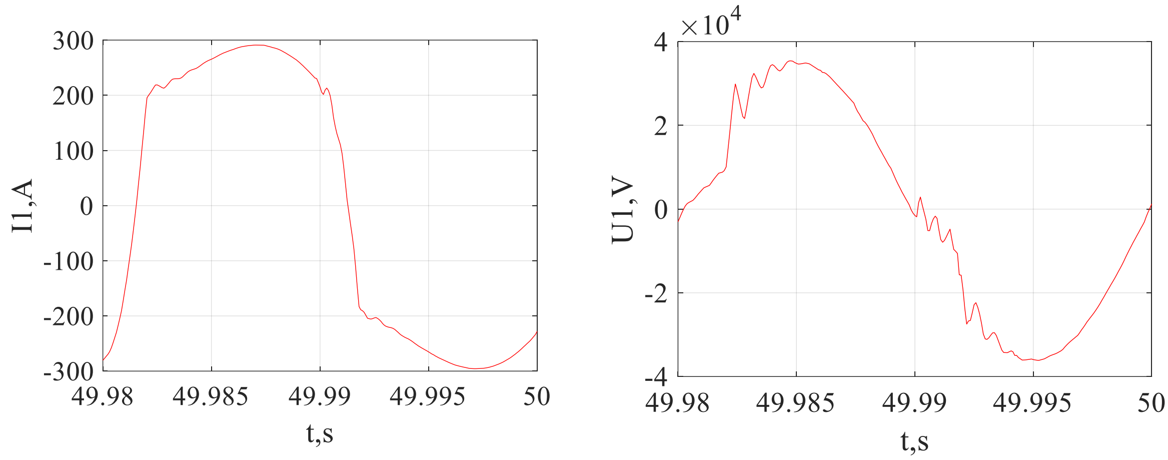

a) b)

Fig. 9. Time diagrams of current (a) and voltage (b) on the primary winding of the traction transformer obtained during the third experiment

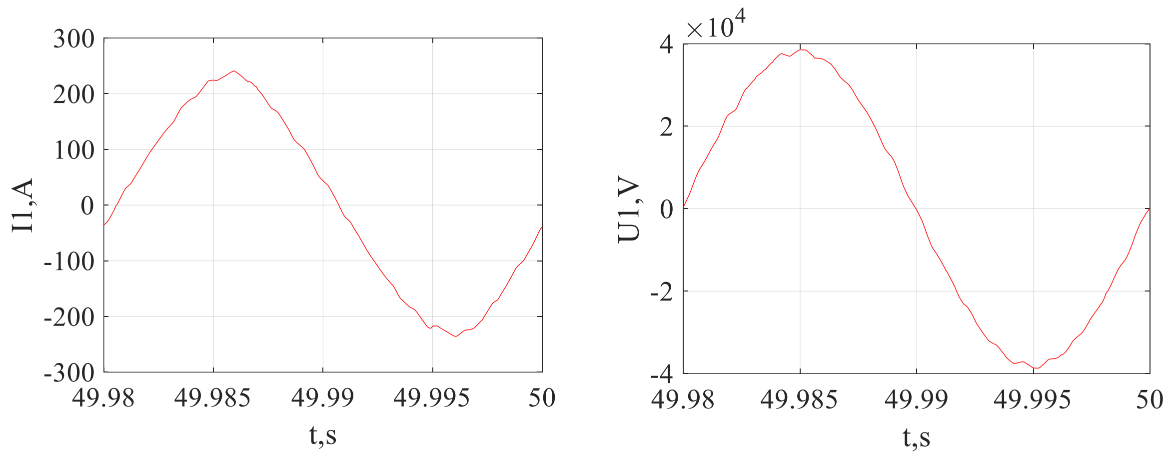

a) b)

Fig. 10. Time diagrams of current (a) and voltage (b) on the primary winding of the traction transformer obtained during the fourth experiment

All four experiments were performed for the nominal mode of operation of the traction drive, maintaining the nominal frequency of the motor shaft of 915 rot/min. Figures 7-10 show the graphs of currents and voltages of the traction transformer primary winding for the steady-state mode.

According to the results obtained, the amplitude-frequency and phase-frequency spectra of currents and voltages of the traction transformer primary winding were obtained in accordance with (15). The number of indications for the period was N=256. Based on the obtained spectral components for the four experiments, the coefficients of power and the total power that was consumed by the electric locomotive from the catenary were calculated.

The locomotive power coefficient upon the disconnected drive of the auxiliary machines was determined using formula of [25]:

$$k_p = \frac{P_{1(1)}}{S}, \qquad (22)$$

where $P_{1(1)}$ is the active power consumed by the traction transformer primary winding at the main frequency of the catenary;

S is the total power consumed by the traction transformer primary winding.

The active power consumed by the traction transformer at the main frequency of the catenary [25, 26] is as follows:

$$P_{1(1)} = I_{1(1)} \cdot U_{1(1)} \cdot cos\left(\varphi_{U_{1(1)}} - \varphi_{I_{1(1)}}\right), \qquad (23)$$

$I_{1(1)}$ is the amplitude of the first harmonics of the current in the primary winding of the traction transformer;
$U_{1(1)}$ is the amplitude of the first harmonics of the voltage at the primary winding of the traction transformer;
$\varphi_{U1(1)}$ is the phase of the first harmonic component of voltage in the primary winding of the traction transformer.

The total power consumed by the traction transformer was determined using formula of [25, 26]:

$$S = \sum_{i=0}^{N} \sqrt{\left(P_{1(i)}\right)^2 + \left(Q_{1(i)}\right)^2}, \qquad (24)$$

where $P_{1(i)}$ is the active power of the *i*-th harmonic component consumed by the primary winding of the traction transformer;
$Q_{1(i)}$ is the reactive power of the *i*-th harmonic component consumed by the primary winding of the track transformer.

The active power of the *i*-th harmonic component consumed by the primary winding of the traction transformer is calculated using the formula from [25, 26]:

$$P_{1(i)} = U_{1(i)} \cdot I_{1(i)} \cdot cos\left(\varphi_{1(i)}\right). \qquad (25)$$

The reactive power of the *i*-th harmonic component consumed by the primary winding of the traction transformer is calculated using the formula from [25, 26]:

$$Q_{1(i)} = U_{1(i)} \cdot I_{1(i)} \cdot sin\left(\varphi_{1(i)}\right), \qquad (26)$$

In formulas (24-26) $U_{1(i)}$ is the amplitude of the i-th harmonic component of voltage in the primary winding of the traction transformer; I1(i) is the amplitude of the i-th harmonic component of current in the primary winding of the traction transformer; φ1(i) is the phase shift between the i-th harmonic components of voltage and current of the primary winding of the traction transformer; N is the number of harmonic components of voltage and current of the primary winding of the traction transformer.

The phase shift between the first harmonic components of voltage and current of the primary winding of the traction transformer was defined by the formula from [25, 26]:

$$\varphi_{1(i)} = \varphi_{U1(i)} - \varphi_{I1(i)}. \qquad (27)$$

The results of the calculation are presented in Table 2.

Table 2

Results of calculations of power coefficients and total power consumed by electric locomotive from the catenary

Parameter	Number of experiment			
	1	2	3	4
Coefficient of power, o.e.	0,85	0,918	0,833	0,912
Total power consumed by electric locomotive from the catenary, kV·A	4886	4525	6543	4643

From Table 2 is seen that the use of the reactive power hybrid compensator in the system of the traction drive increases the coefficient of power of the traction driver and hence decreases the total power consumed by the electric locomotive from the catenary.

The most marked here is the effect of the use of the reactive power hybrid compensator upon the nonstationary nondeterministic process of the change in voltage of the catenary. Thus, in the traction drive in the absence of the compensator, at the nonstationary nondeterministic process of the voltage change in the catenary, the total power that was consumed by the electric locomotive from the catenary increased by 33.9 % compared to the case of the stationary deterministic process of the change in the voltage of the catenary. A similar comparison for the traction drive in the presence of the reactive power compensator showed that the total power increase that was consumed by the electric locomotive from the network was 2.6 %.

CONCLUSIONS

В работе предложена модель гибридного In this work, the reactive power compensator model was offered with adaptation of the monitoring system operation to the supply main voltage parameters. To solve this problem:

-the algorithm of the monitoring system operation of the compensator active part was developed;

-the monitoring system structure of the compensator active part was developed;

-the compensator passive part elements were calculated;

-the modeling was fulfilled;

-the simulation modeling of the traction drive operation of VL-80k locomotive with the reactive power compensation was fulfilled;

-for the nominal mode of the electric locomotive operation at the nominal value of frequency of the motor shift rotation, four experiments were performed. The first consisted of obtaining the time current and voltage diagrams of the primary winding of the traction transformer for the traction drive with no compensator under condition that the process of voltage change in the catenary is a stationary deterministic process. The second was to obtain time diagrams of current and voltage of the primary winding of the traction transformer under the same conditions of voltage changing in the catenary, but with a reactive power compensator. The third had to obtain time diagrams of current and voltage of the primary winding of the traction transformer with no compensator under condition that the process of changing voltage in the catenary is a nonstationary nondeterministic process. The fourth one was aimed at obtaining the time diagrams of current and voltage of the primary winding of the traction transformer with a compensator in condition that the process of changing voltage in the catenary is a nonstationary and nondeterministic process.

-according to the diagrams obtained for the steady-state mode the amplitude-frequency and phase-frequency spectra of currents and voltages , using which we calculated the locomotive power coefficient and the total power consumed by the electric locomotive from the network. The analyses of the results showed that the reactive power compensator use in the traction drive system increases the traction drive power coefficient, decreasing thus the total power that is consumed by the locomotive from the catenary.

REFERENCES

[1] Hanafy A. M., Hebala O. M., Hamad, M. S. Power Quality Issues in Traction Power Systems. In *2021 22nd International Middle East Power Systems Conference (MEPCON)*, 2021, pp. 188-193. IEEE. Available at: doi: 10.1109/MEPCON50283.2021.9686222. (Accessed october 15, 2022).

[2] Jin M., Yang Y., Yang J., Wu M., Xie G., Song K. Propagation Characteristics and Identification of High-Order Harmonics of a Traction Power Supply System. *Energies*, 2022, vol. 15, no 15, pp. 5647-5661. Available at: doi: 10.3390/en15155647. (Accessed october 15, 2022).

[3] Martins A. P., Rodrigues P., Hassan M., Morais V. A. Voltage Unbalance, Power Factor and Losses Optimization in Electrified Railways Using an Electronic Balancer. *Electricity*, 2021, vol. 2, no 4, pp. 554-572. Available at: doi: 10.3390/electricity2040032. (Accessed october 15, 2022).

[4] Li T., Shi Y. Power Quality Management Strategy for High-Speed Railway Traction Power Supply System Based on MMC-RPC. *Energies*, 2022, vol. 15, no 14, pp. 5205-5224. Available at: doi: 10.3390/en15145205. (Accepted October 10, 2022).

[5] Zhu J., Hu H., He Z., Guo X., Pan W. A power-quality monitoring and assessment system for high-speed railways based on train-network-data center integration. *Railway Engineering Science*, 2021, vol. 29, no 1, pp. 30-41. Available at: doi: 10.1007/s40534-020-00229-4. (Accessed october 15, 2022).

[6] Wu S., Wu M., Wang Y. A novel co-phase power-supply system based on modular multilevel converter for high-speed railway AT traction power-supply system. *Energies*, 2021, vol. 14, no 1, pp. 253-269. Available at: doi: 10.3390/en14010253. (Accessed october 15, 2022).

[7] Arabahmadi M., Banejad M., Dastfan A. Hybrid compensation method for traction power quality compensators in electrified railway power supply system. *Global Energy Interconnection*, 2021, vol. 5, no 2, pp. 158-168. Available at: doi: 10.1016/j.gloei.2021.05.008. (Accessed October 15, 2022).

[8]Kostin M., Nikitenko A., Mishchenko T., Shumikhina L. Electrodynamics of Reactive Power in the Space of Inter-Substation Zones of AC Electrified Railway Line. *Energies*, 2021, vol. 14, no 12, pp. 3510-3528. Available at: doi: 10.3390/en14123510. (Accessed October 15, 2022).

[9] Li G., Hu B., Shao C. Development of Cascade H Bridge SVG. In *2021 IEEE 16th Conference on Industrial Electronics and Applications (ICIEA)*, 2021, pp. 2053-2057. IEEE. Available at: doi: 10.1109/ICIEA51954.2021.9516073. (Accessed October 15, 2022).

[10] Moore T., Schmid, F., Tricoli P. Voltage transient management for Alternating Current trains with vacuum circuit breakers. *IET Electrical Systems in Transportation*, 2021, vol. 12, no 1, pp. 1-14. Available at: doi: 10.1049/els2.12034. (Accessed October 15, 2022).

[11] Misra B., Tripathy P., Mohanty R., Sahoo S. R., Nayak, B. Performance Analysis of an Adaptive Hysteresis Band Current Controller based Active Power Filter. In *2022 Second International Conference on Advances in Electrical, Computing, Communication and Sustainable Technologies (ICAECT)*, 2021, pp. 1-4. Available at: doi: 10.1109/ICAECT54875.2022.9807992. (Accessed October 15, 2022).

[12] Mariscotti A., Sandrolini L. Detection of harmonic overvoltage and resonance in AC railways using measured pantograph electrical quantities. *Energies*, 2021, vol. 14, no 18, pp. 5645. Available at: doi: 10.3390/en14185645. (Accessed October 15, 2022).

[13] Lin J., Hu S., Li Y., Luo L., Zhang J., Cao Y., Gao B., Yu J., Zhou, F. A Novel Power Programming Strategy for Railway Power Regulation with Dynamic Exploration. *IEEE Transactions on Smart Grid*, 2022, vol. 13, no 4, pp. 2798. Available at: doi: 10.1109/TSG.2022.3160500. (Accessed October 15, 2022).

[14] Simiyu P., Davidson I. E. MVDC railway traction power systems; state-of-the art, opportunities, and challenges. *Energies*, 2021, vol. 14, no 14, pp. 4156. Available at: doi: 10.3390/en14144156. (Accessed October 15, 2022).

[15] Mohammed M. K., Mohamad Niyef S., Hamodat Z. SVC Based Smart Grid Management of Renewable Energy Resources. In *2022 International Congress on Human-Computer Interaction, Optimization and Robotic Applications (HORA)*, 2022, pp. 1-4. Available at: 10.1109/HORA55278.2022.9799953. (Accessed October 15, 2022).

[16] Ma Q., Wang H., Luo P., Peng Y., Li Q. Ultra-short-term Railway traction load prediction based on DWT-TCN-PSO_SVR combined model. *International Journal of Electrical Power & Energy Systems*, 2022, vol. 135, pp. 107595. Available at: doi: 10.1016/j.ijepes.2021.107595. (Accepted October 17, 2022).

[17] Bellè A., Zeng Z., Duval C., Sango M., Barros A. Modeling and vulnerability analysis of interdependent railway and power networks: Application to British test systems. *Reliability Engineering & System Safety*, 2022, vol. 217, pp. 108091. Available at: doi: 10.1016/j.ress.2021.108091. (Accessed October 15, 2022).

[18] Goolak S., Tkachenko V., Bureika G., Vaičiūnas G. Method of spectral analysis of traction current of AC electric locomotives. *Transport*, 2020, vol. 35, no 6, pp. 658-668. Available at: doi: 10.3846/transport.2020.14242. (Accessed October 17, 2022).

[19] Nicolae P. M., Nicolae I. D., Nuca I., Nicolae, M. S. Determination of Electromagnetic Noise from a Power Supply Substation of Railway Traction Systems. In *2022 IEEE International Symposium on Electromagnetic Compatibility & Signal/Power Integrity (EMCSI)*, 2022, pp. 619-624. IEEE. Available at: doi: 10.1109/EMCSI39492.2022.9889567. (Accessed October 20, 2022).

[20] Usha S., Tiwari S., Kundu U. Robust speed control of inverter fed parallel connected induction motors for electric vehicle traction applications. *Materials Today: Proceedings*, 2022, vol. 66, no 3, pp. 975-981. Available at: doi: 10.1016/j.matpr.2022.04.774. (Accessed October 20, 2022).

[21] Che Y., Wang X., Lv X., Lin H. Correlation analysis of traction load sequences based on optimal delay method. *International Journal of Electrical Power & Energy Systems*, 2022, vol. 142, pp. 108356. Available at: doi: 10.1016/j.ijepes.2022.108356. (Accessed October 20, 2022).

[22] Liu W., Zhang J., Wang H., Wu T., Lou Y., Ye X. Modified AC/DC unified power flow and energy-saving evaluation for urban rail power supply system with energy feedback systems. *IEEE Transactions on Vehicular Technology*, 2022, vol. 70, no 10, pp. 9898-9909. Available at: doi: 10.1109/TVT.2021.3104309. (Accessed October 20, 2022).

[23] Kaleybar H. J., Brenna M., Foiadelli F. Dual-loop generalized predictive control method for two-phase three-wire railway active power quality controller. *Transactions of the Institute of Measurement and Control*, 2021, vol. 43, no 1, pp. 88-101. Available at: doi: 10.1177/0142331220932470. (Accessed October 25, 2022).

[24] Roudsari H. M., Jamali S., Jalilian A. Dynamic modeling, control design and stability analysis of railway active power quality conditioner. *Electric Power Systems Research*, 2018, vol. 160, pp. 71-88. Available at: doi: 10.1016/j.epsr.2018.01.027. (Accessed October 15, 2022).

[25] Zarifyan A. A., Talakhadze N. V. Comparative research of electrical energy transformation processes in locomotive traction drives with asynchronous motors and series-wound brushed DC motors. In *Journal of Physics: Conference Series*, 2021, vol. 2131, no. 4, pp. 042079. IOP Publishing. Available at: doi: 10.1088/1742-6596/2131/4/042079. (Accessed October 15, 2022).

[26]Iksar E., Nazirova Z. Improving the energy efficiency of traction motors taking into account the assessment of the thermal condition. *International Journal of Advanced Logistics*,

Transport and Engineering, 2022, vol. 2, no. 2, pp. 14-19. Available at: doi: 10.52167/2790-5829-2022-2-2-14-19. (Accessed October 15, 2022).

Information about authors

Goolak Sergey, candidate of technical sciences, Kiev Institute of Railway Transport of the State University of Infrastructure and Technology. Field of scientific interests – mathematical modeling of control systems for traction drives of electric locomotives.
E-mail:
goolak@gmail.com

Kyrychenko Myhailo candidate of technical sciences, Kyiv National University of Construction and Architecture. Field of scientific interests – mathematical modeling of thermodynamic processes.
E-mail:
kirichenkom@ukr.net

Tkachenko Victor, doctor of technical sciences**,** Kiev Institute of Railway Transport of the State University of Infrastructure and Technology. Field of scientific interests – increasing the energy efficiency of traction drives of electric locomotives.
E-mail:
v.p.tkachenko.detut@gmail.com

Kozlov Serhii, candidate of technical sciences, National Technical University «Kharkiv Polytechnic Institute». Field of scientific interests – increasing the efficiency of operation of electrical network facilities.
E-mail:
ksser300@gmail.com